Plate coupling across the northern Manila subduction zone deduced from mantle lithosphere buoyancy

Chung-Liang Lo[a,*], Wen-Bin Doo[b], Hao Kuo-Chen[a], Shu-Kun Hsu[a,b]

[a] Department of Earth Sciences, National Central University, Taiwan
[b] Center for Environmental Studies, National Central University, Taiwan

ABSTRACT

The Manila subduction zone is located at the plate boundary where the Philippine Sea plate (PSP) moves northwestward toward the Eurasian plate (EU) with a high convergence rate. However, historically, no large earthquakes greater than Mw7 have been observed across the northern Manila subduction zone. The poorly understood plate interaction between these two plates in this region creates significant issues for evaluating the seismic hazard. Therefore, the variation of mantle lithospheric buoyancy is calculated to evaluate the plate coupling status across the northern Manila subduction zone, based on recently published forward gravity modeling constrained by the results of the P-wave seismic crustal structure of the TAIGER (Taiwan Integrated Geodynamic Research) project. The results indicate weak plate coupling between the PSP and EU, which could be related to the release of the overriding PSP from the descending EU's dragging force, which was deduced from the higher elevation of the Luzon arc and the fore-arc basin northward toward the Taiwan orogen. Moreover, serpentinized peridotite is present above the plate boundary and is distributed more widely and thickly closer to offshore southern Taiwan orogen. We suggest that low plate coupling may facilitate the uplifting of serpentinized mantle material up to the plate boundary.

1. Introduction

The Taiwan orogen, one of the world's most active mountain belts, is shaped by the collision between the Philippine Sea plate (PSP) and the Eurasian plate (EU) (Biq, 1981; Chai, 1972; Teng, 1990). To the south, the crust of the South China Sea (SCS) is subducting eastward beneath the PSP along the Manila trench, whereas the overriding Luzon arc (LA) obliquely collides with the EU continental margin (Hsu and Sibuet, 1995; Sibuet and Hsu, 2004; Wu et al., 1997). The Manila trench, which stretches from the Philippine archipelago to offshore southwestern Taiwan, is currently a less seismically active plate boundary between the SCS and the PSP with infrequent seismicity in the northern subduction zone (Fig. 1). The Global CMT earthquake catalogue (http://www.globalcmt.org/) has recorded previously occurring Mw6 earthquakes, but no large earthquakes greater than Mw7 since the 1960s (Dziewonski et al., 1981; Ekström et al., 2012). This observation lends credence to evaluating the seismic hazard potential of this subduction zone, which Hsu et al. (2012) proposed in view of a nuclear power plant on the southern tip of Taiwan.

As immediately adjacent to the active Taiwan mountain building area, offshore southern Taiwan is considered as a transition zone linking the Manila subduction zone to the arc-continent collision on-land Taiwan. Hyperextended continental crust of EU margin subduction and accreted transitional crust has been documented by the TAIGER project in this region (Lester et al., 2013; McIntosh et al., 2013; Eakin et al., 2014). The subducting crust contains both oceanic (Taylor and Hayes, 1980; Briais et al., 1993) and hyperextended continental materials (McIntosh et al., 2013) resulting the arc-continental collision model in southern Taiwan. In addition, from the GPS inversions, Hsu et al. (2012, 2016) found low plate coupling along the Manila subduction zone in the Luzon island section. However, the spatial distribution of the GPS networks in the northern Manila convergent zone is sparse due to the limited land coverage, thus the plate coupling status there is less well-constrained.

Knowing the crustal structure helps to evaluate the fundamental physical properties of the lithosphere, especially for the plate boundary region. The seismic velocities below the accretionary prism and mantle wedge are important physical properties for understanding the contact zone, where the overriding plate is coupled to the descending slab and is pulled down to a region where the overriding plate floats freely on the asthenosphere. The lithospheric structure also reflects the buoyancy of the lithospheric layer, which provides separated crustal and mantle
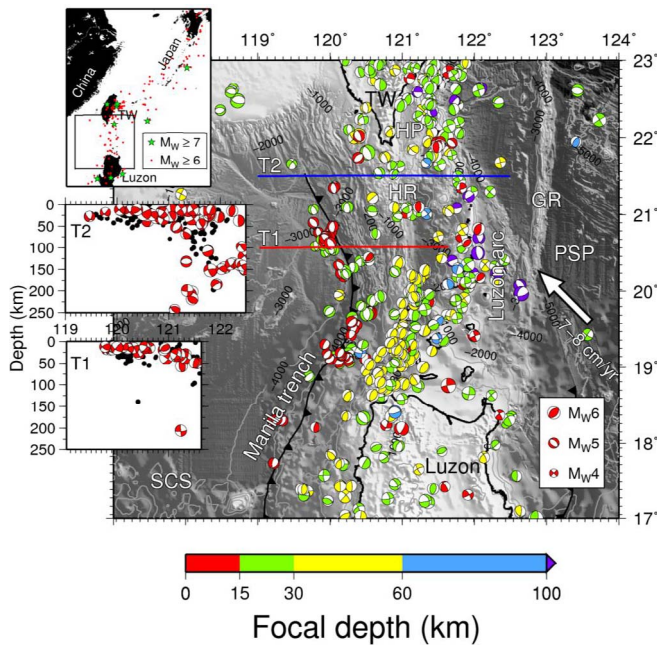
Fig. 1. The tectonic setting in the northern Manila subduction zone off the southern Taiwan region. The seismic focal mechanisms were adopted from the Global CMT project data catalogue. T1 and T2 are seismic profiles from ocean bottom seismometers (OBS), which were collocated with multi-channel seismic reflection (MCS) data sets from the TAIGER project. The profiles also show the lateral projection of the focal mechanisms within 50 km of each side. The black dots in the two profiles are earthquakes from USGS earthquake archives. GR: Gagua ridge; HP: Hengchun peninsula; HR: Hengchun ridge; PSP: Philippine Sea Plate; SCS: South China Sea; TW: Taiwan.

lithospheric contributions to the topography. This relationship can indicate the extent of the plate coupling across the convergent plate region by considering residual topography changes (Gvirtzman and Nur, 1999; Lachenbruch and Morgan, 1990). When plate coupling is strong, the descending slab seems almost fixed in the mantle. When plate coupling is weak, the overriding plate is decoupled (or detached) from the subducted plate and the wedged asthenospheric material propagates upward toward the plate contact zone between the two plates. The gravitational force acting on the descending slab works against the negative suction pressure in the subduction mantle wedge (Nur et al., 1993; Dvorkin et al., 1993), and the mantle lithospheric buoyancy (H_m) will subsequently change. Therefore, the variations in mantle lithosphere buoyancy across the subduction zone are related to changes in the plate coupling state between the overriding and subducting plates (Gvirtzman and Nur, 1999). In general, the normal H_m ranges from -1.5 to -2.5 km in the passive margin (Gvirtzman and Nur, 1999). For strong plate coupling, the variation in H_m is relatively minor, because the subducting slab may have undergone strong suction, which prevents the slab from sinking as fast, e.g., the Andean-type subduction zone (Gvirtzman and Nur, 1999) and the southernmost Ryukyu subduction zone (Hsu, 2001). In contrast, the H_m curve may show more undulation, which represents weak plate coupling, e.g., the Calabria peninsula in the southern Tyrrhenian subduction zone (Italy) (Gvirtzman and Nur, 1999). The H_m curves across the Bonin and Kurile arcs show other cases of intermediate coupling (Fig. 4).

In this study, we calculated H_m curves using an empirical relationship between P-wave velocities and densities to obtain density structures (Doo et al., 2015) for two seismic profiles in southern offshore Taiwan from the TAIGER project (T1 and T2 in Fig. 1) based on the available lateral extent of the plate contact zones (Eakin et al., 2014). We estimated the plate coupling status and then examined the possibility of large earthquakes (Mw > 7) and interpret the crustal-scale tectonic structures in the northern Manila subduction zone between the PSP and the SCS.

2. The crustal and mantle lithospheric buoyancies

In isostatic equilibrium, the mean elevation of a region can be expressed as follows:

$$\varepsilon = a(H_c + H_m - H_0), \tag{1}$$

$$a = 1 \text{ for } \varepsilon \geqslant 0$$

$$a = \frac{\rho_a}{\rho_a - \rho_w} \text{ for } \varepsilon < 0$$

where ε is the surface elevation; ρ_a and ρ_w are the densities of the asthenosphere and water, respectively; and $H_0 \approx 2.4$ km is a reference constant for the buoyant height of the sea level at the mid-ocean ridge, which is associated with the densities in Eq. (1) (Lachenbruch and Morgan, 1990). H_c and H_m are the buoyancies of the crust and the mantle lithosphere, respectively:

$$H_c = \frac{1}{\rho_a}(\rho_a - \rho_c)L_c, \tag{2}$$

$$H_m = \frac{1}{\rho_a}(\rho_a - \rho_m)L_m, \tag{3}$$

where ρ_c, ρ_m, L_c and L_m are the densities and thicknesses of the crust and mantle lithosphere, respectively.

The above relationships assume isostatic equilibrium, in which the lithosphere is freely floating on the asthenosphere. Therefore, the topography is theoretically influenced by the crust and mantle lithosphere's thickness, and the residual topography will be mostly attributed to the H_m if H_c has been solved from Eq. (1). However, these relationships should be applied with caution when adapted to the subduction zone, as the topography will be lowered because of drag from a descending slab or uplifted by ascending hot asthenospheric material. Thus, the residual topography, defined as the observed topography minus the calculated contribution of the crust (Gvirtzman and Nur, 1999; Lachenbruch and Morgan, 1990), must be considered. The residual topography in the subduction zone is the result of drag forces from descending slabs, uplift from ascending asthenospheric material, and the local H_m. The dynamic dragging force from the subducting slab will lower the topography near the plate boundary below that of a statically balanced floating plate. Similarly, the upwelling asthenospheric material below the overriding plate will heat and, thus, thin the mantle lithosphere dynamically toward the plate contact, which will raise the topography. Therefore, the residual topography in these areas reflects the contribution from the non-crustal forces and depends on the status of plate coupling, which is revealed by the H_m anomaly (Gvirtzman and Nur, 1999).

3. Gravity forward modeling result and crustal structure

The structure of the crust is required to calculate H_c. Eakin et al. (2014) have produced two long E-W multi-channel seismic (MCS) data sets associated with ocean bottom seismometer (OBS) profiles at 20.5 (T1) and 21.5 (T2) degrees north latitude (see Fig. 1). Both profiles reveal clear crustal velocity structures along the SCS and PSP crust across the northern Manila subduction zone, except in the deeper areas under the accretionary prisms. Forward gravity modeling was performed along these two profiles to verify that the structures are compatible with the gravity data (Doo et al., 2015) and are in agreement with the observed gravity anomalies (Hsu et al., 1998). The total crustal buoyancy was calculated according to the density model of Doo et al. (2015) (Figs. 2c and 3c), and the buoyancy of the mantle lithosphere was calculated from equations 2 and 3 (Figs. 2a, 3a, and 4).

4. Discussion

Over 10 km of sedimentary and accretionary prisms lie on top of the
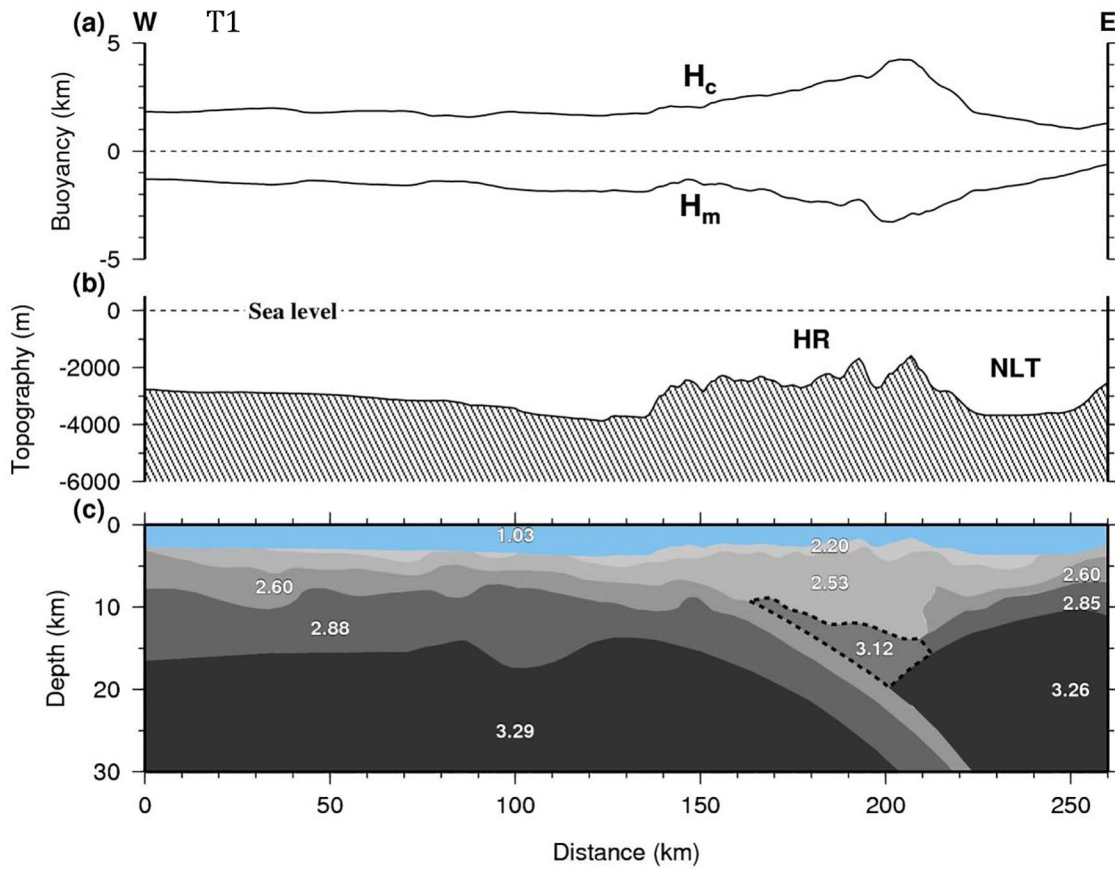
Fig. 2. The transect T1 across the northern Manila subduction zone displays (a) the calculated buoyancy results of crust and mantle lithosphere from forward gravity modeling (see details in the text and in Doo et al., 2015); (b) the elevation along the profile; and (c) the crustal and mantle density structures that were validated from the forward gravity modeling results; the area in the black dashed line underlying the accretionary prism is the assumed serpentinized material. HR: Hengchun ridge; NLT: northern Luzon trough.
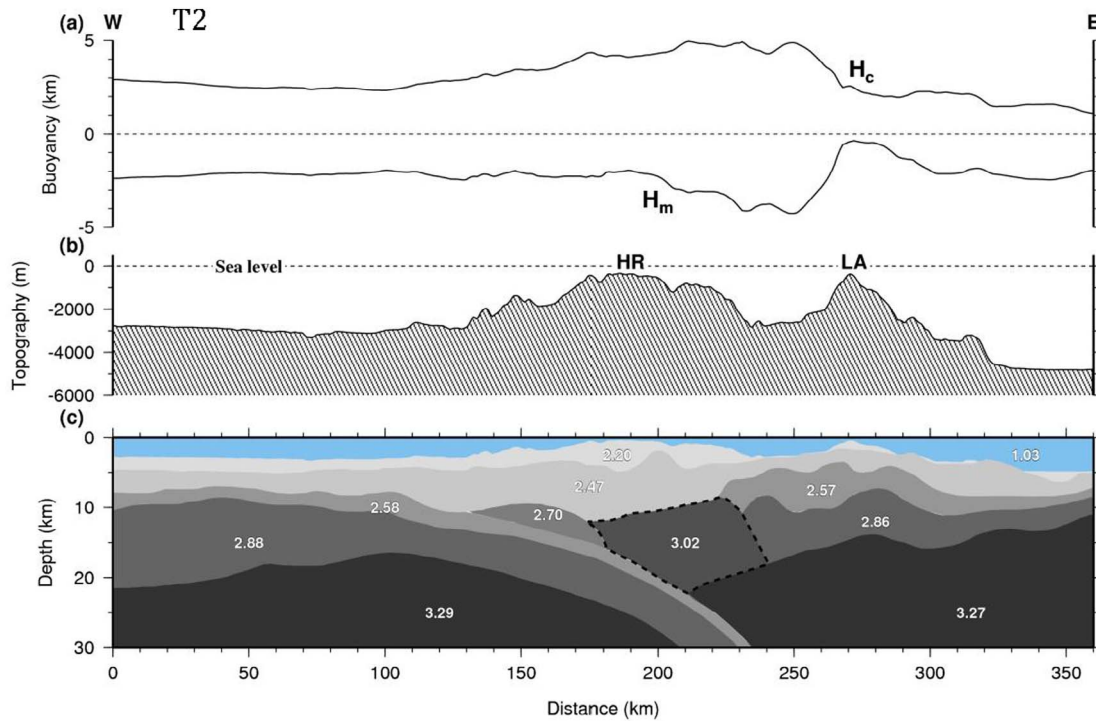
Fig. 3. The transect T2 across the northern Manila subduction zone, with similar annotations to those in Fig. 2. The elevation of the Luzon arc and accretionary prism in (b) is higher than that in Fig. 2b. Meanwhile, the extent of the serpentinized material in the high-density anomaly, which is enclosed with a black dashed line, is noticeably wider than that in Fig. 2c. HR: Hengchun ridge; LA: Luzon arc.
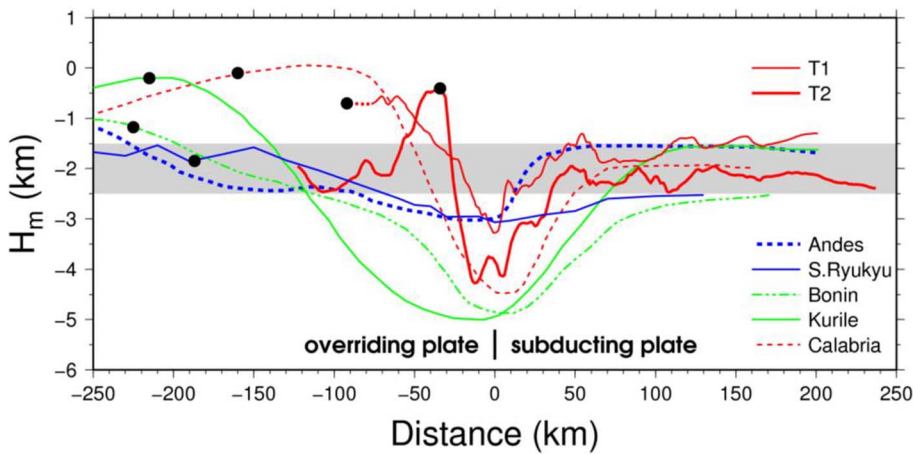
Fig. 4. The mantle lithospheric buoyancy H_m variations for several different subduction zones were calculated. The variation in the Andes anomaly is weak and wide, and that in the Calabria anomaly is large and narrow. The Izu-Bonin and Kurile anomalies are intermediate in type. The anomaly in southernmost Ryukyu varies slightly. The T1 and T2 undulations across the northern Manila subduction zone are more severe than the others, especially for the T2 profile, which behaves violently because of the narrow fore-arc region. The plate coupling status is shown in red for weak, green for intermediate and blue for strong plate coupling, respectively. The gray band zone (-2.0 ± 0.5) represents normal variations in H_m. The black dots are the positions of arcs.

plate contact zone in both profiles T1 and T2 (Figs. 2c and 3c), which indicates that the SCS had a strong coupling with the PSP, verified by evidence of the fore-arc area being pulled down during periods of subsidence. However, the H_m curve variation across the northernmost Manila trench is large, which implies that the plate coupling is currently not strong. The variations in both the H_m curves exceed the normal plate coupling range: the southern T1 profile H_m varies from -3.3 at the plate boundary to -0.5 km at the (fore-) arc, and the northern T2 profile H_m varies from -4.3 to -0.3 km (Figs. 2a and 3a). Among all the listed subduction zones, the maximum/minimum H_m values of T2 and its undulation pattern are closest to those observed at the Calabria H_m curve, even over a very short distance, which suggests that the coupling between the SCS and PSP is very weak (Fig. 4). This observation also agrees with the elevations of the LA and the fore-arc basin in profile T2, which are higher than those in T1 (see Figs. 3b and 2b), and implies that the downward slab dragging force is gradually diminishing (Gvirtzman and Nur, 1999).

Moreover, the down-dip tendency of H_m toward the plate contact zone in T2 is steeper than that in T1 and in other subduction zones. The H_m transition in the Andean curve is weaker and wider than that in the Calabria curve because a large portion of the overriding plate is coupled to the slab. In contrast, the sharp transition across the northern Manila subduction zone could indicate a very narrow range of plate coupling, which also suggests the narrow coupled range between overriding and subducting plate implying that the former can be released relative easily. Even though it is not in the case of the Calabrian environment, but both the coupling statuses are similar (Gvirtzman and Nur, 1999). Besides, the H_m value in the fore-arc region is close to zero, which indicates that the mantle lithosphere is drastically thinner and that will decrease the negative mantle buoyancy and lead to uplift of the fore-arc northward.

According to gravity modeling results (Doo et al., 2015), the T1 profile shows that the density of the overriding crust above the plate interface is slightly higher than that of the ambient normal crust (Fig. 2c). Similar high-density material still appears in the plate interface in profile T2 and occupies an even thicker and wider range (Fig. 3c). Serpentinization results from chemical reaction of water released from the descending oceanic slab and peridotites in the mantle wedge; serpentinized rock is less dense than ambient mantle material (Coleman, 1971; Gerya, 2011; Hacker and Gerya, 2013). Therefore, serpentinization probably occurs in the fore-arc mantle wedge and then serpentinized rock exhumes up to the lower crust into the plate contact zone due to self-buoyancy driving (Doo et al., 2015; Gerya et al., 2002; Hyndman and Peacock, 2003). Pilchin (2005) argued that there needs an external force presence for the exhumation of high-grade rocks to the surface, and it cannot be accomplished by buoyancy alone. Thus, weak plate coupling could provide as a reasonable external force. In this case, the narrower range coupled between plates, the stronger the plate

decoupling, and the drastic mantle thinning in the arc region that will make more space in the mantle wedge for asthenospheric thermal intrusion, which facilitates the effects of exhumation serpentinizaed fore-arc mantle.

Though it is not an absolute relationship, the relative low seismicity in the northern Manila subduction zone also indicates that the plate coupling at present day is not as strong as expected (Lin et al., 2015). No large Mw ≥ 7 earthquakes have been observed in this area, although one did occur offshore of southeastern Taiwan (Fig. 1). A few earthquakes displayed normal focal mechanisms on the western side of the Hengchun ridge (HR), but others between the HR and the LA have diverse focal mechanisms (Fig. 1). Most earthquakes are seldom both greater than Mw6 and deeper than 30 km in this region up to east of the LA segment, where seismicity is more active because of the collision between the LA and Taiwan. The seismicity along the two profiles also shows that the geometry of the subducting SCS slab in T2 is steeper than that in T1 (Eakin et al., 2014). Tan (2017) showed that the slab dip is affected by the down-dip extent and the thickness of mantle serpentinization. From our result, the serpentinized mantle rocks in both T1 and T2 are in the same depth extent, but the amount in T2 is larger than that in T1, which is consistent with Tan's result (2017). Based on the preceding discussion, the SCS descending slab bends more steeply when approaching Taiwan to the north because the collision between the LA and Taiwan becomes stronger, which weakens the coupling between the overriding PSP and the subducting SCS crust. Moreover, the lack of Mw ≥ 7 and the scarcity Mw ≥ 6 earthquakes in the record suggest that the plate coupling here is not strong. Compared to the southernmost Ryukyu subduction zone to the east of Taiwan, the down-dip tendency and undulation of H_m shows that plate coupling is weaker in the northern Manila subduction zone to the south of Taiwan (Fig. 4). This observation also is in agreement with the more active seismicity to the east of Taiwan than to the south.

This study proposes a simple model that combines seismicity distributions, gravity forward modeling and the calculation of mantle lithospheric buoyancy across the northern Manila subduction zone. The plate coupling between the SCS and the PSP in the northern Manila subduction zone remains unclear still where the LA is experiencing colliding with the passive EU margin. However, the subducting slab shows bending more steeply because of the stronger collision close to Taiwan, which reduces the coupling portion between the plates, decreases the downward dragging force and increases the mantle wedge window along with the thermal effects of the asthenospheric intrusion, and results in the uplift of the fore-arc region. Meanwhile, dewatering from the descending slab produces serpentinization in the mantle wedge, and the serpentinized rock then uplifts to the plate contact zone because its lower density than that of the ambient mantle material. The crustal structure is consistent with the gravity anomaly results from gravity modeling and reveals that serpentinization is stronger

northward. This phenomenon is likely a response to similar density material being distributed throughout a smaller region in T1 and a wider region in T2. Finally, the undulation of the H_m curve demonstrates that the plate coupling in the northern Manila subduction zone is weaker.

5. Conclusion

We propose that the strength of the plate coupling across the northern Manila subduction zone is weak based on calculations of the variations in mantle lithospheric buoyancy. Steep H_m curves show that plate coupling decreases northward toward the Taiwan orogen. This observation is consistent with the topography of the fore-arc region of the Luzon arc, which is higher toward Taiwan and implies that the release of the slab dragging force from the descending slab causes the overriding plate to gradually rebound. The inactive seismicity and the scarcity of large earthquakes in this area also support the idea of weak plate coupling. Furthermore, the results of gravity forward modeling suggest that serpentinized peridotite-like material exists in the plate contact zone, which fits the observed gravity anomaly. Dehydration and serpentinization occurs in the SCS subducting slab and becomes stronger with steeper slab subduction toward the Taiwan orogen. Due to weak plate coupling, the serpentinized peridotite in the mantle wedge could uplift to the plate interface because its density is smaller than the ambient mantle density. The steeper the slab, the more easily the asthenosphere can flow into the mantle wedge, which will heat the slab. Heating the slab facilitates the dehydration of the slab surface and serpentinization of the mantle material, which facilitates the uplifting of the serpentinized rock. This concept is supported by the observation that the serpentinized rock occupies a wider and thicker range in the T2 profile than in the T1 profile.

Acknowledgements

References

Biq, C., 1981. Collision. Taiwan-style. Mem. Geol. Soc. China 4, 91–102.

Briais, A., Patriat, P., Tapponnier, P., 1993. Updated interpretation of magnetic anomalies and seafloor spreading stages in the South China Sea: implications for the Tertiary tectonics of Southeast Asia. J. Geophys. Res. 98, 6299–6328. http://dx.doi.org/10.1029/92JB02280.

Chai, B.H.T., 1972. Structure and tectonic evolution of Taiwan. Am. J. Sci. 272, 389–422. http://dx.doi.org/10.2475/ajs.272.5.389.

Coleman, R.G., 1971. Petrologic and geophysical nature of serpentinites. Geol. Soc. Am. Bull. 82, 897–918. http://dx.doi.org/10.1130/0016-7606(1971) 82(897:PAGNOS)2.0.CO;2.

Doo, W.-B., Lo, C.-L., Kuo-Chen, H., Brown, D., Hsu, S.-K., 2015. Exhumation of serpentinized peridotite in the northern Manila subduction zone inferred from forward gravity modeling. Geophys. Res. Lett. 42. http://dx.doi.org/10.1002/2015GL065705.

Dvorkin, J., Nur, A., Mavko, G., Ben Avraham, Z., 1993. Narrow subducting slabs and the origin of backarc basins. Tectonophysics 227, 63–79. http://dx.doi.org/10.1016/0040-1951(93)90087-Z.

Dziewonski, A.M., Chou, T.-A., Woodhouse, J.H., 1981. Determination of earthquake source parameters from waveform data for studies of global and regional seismicity. J. Geophys. Res. 86, 2825–2852. http://dx.doi.org/10.1029/JB086iB04p02825.

Eakin, D.H., McIntosh, K.D., Van Avendonk, H.J.A., Lavier, L., Lester, R., Liu, C.S., Lee, C.S., 2014. Crustal-scale seismic profiles across the Manila subduction zone: the transition from intraoceanic subduction to incipient collision. J. Geophys. Res. 119, 1–17. http://dx.doi.org/10.1002/2013JB010395.

Ekström, G., Nettles, M., Dziewonski, A.M., 2012. The global CMT project 2004–2010: centroid-moment tensors for 13,017 earthquakes. Phys. Earth Planet. Inter. 200–201, 1–9. http://dx.doi.org/10.1016/j.pepi.2012.04.002.

Gerya, T.V., 2011. Future directions in subduction modeling. J. Geodyn. 52, 344–378. http://dx.doi.org/10.1016/j.jog.2011.06.005.

Gerya, T.V., Stöckhert, B., Perchuk, A.L., 2002. Exhumation of high-pressure metamorphic rocks in a subduction channel: a numerical simulation. Tectonics 21. http://dx.doi.org/10.1029/2002TC001406.

Gvirtzman, Zohar, Nur, A., 1999. Plate detachment, asthenosphere upwelling, and topography across subduction zones. Geology 27, 563–566. http://dx.doi.org/10.1130/0091-7613(1999) 027<0563:PDAUAT>2.3.CO;2.

Hacker, B.R., Gerya, T.V., 2013. Paradigms, new and old, for ultrahigh-pressure tectonism. Tectonophysics 603, 79–88. http://dx.doi.org/10.1016/j.tecto.2013.05.026.

Hsu, S.-K., 2001. Lithospheric structure, buoyancy and coupling across the southernmost Ryukyu subduction zone: an example of decreasing plate coupling. Earth Planet. Sci. Lett. 186, 471–478. http://dx.doi.org/10.1016/S0012-821X(01)00261-8.

Hsu, S.-K., Liu, C.-S., Shyu, C.-T., Liu, S.-Y., Sibuet, J.-C., Lallemand, S., Wang, C.-S., Reed, D., 1998. New gravity and magnetic anomaly maps in the Taiwan-Luzon region and their preliminary interpretation. Terr. Atmos. Ocean. Sci. 9, 509–532.

Hsu, S.-K., Sibuet, J.-C., 1995. Is Taiwan the result of arc – continent or arc-arc collision? Earth Planet. Sci. Lett. 136, 315–324. http://dx.doi.org/10.1016/0012-821X(95)00190-N.

Hsu, Y.-J., Yu, S.-B., Song, T.-R.A., Bacolcol, T., 2012. Plate coupling along the Manila subduction zone between Taiwan and northern Luzon. J. Asian Earth Sci. 51, 98–108. http://dx.doi.org/10.1016/j.jseaes.2012.01.005.

Hsu, Y.-J., Yu, S.-B., Loveless, J.P., Bacolcol, T., Solidum, R., Luis Jr., A., Pelicano, A., Woessner, J., 2016. Interseismic deformation and moment deficit along the Manila subduction zone and the Philippine Fault system. J. Geophys. Res. Solid Earth 121. http://dx.doi.org/10.1002/2016JB013082.

Hyndman, R.D., Peacock, S.M., 2003. Serpentinization of the forearc mantle. Earth Planet. Sci. Lett. 212, 417–432. http://dx.doi.org/10.1016/S0012-821X(03)00263-2.

Lachenbruch, A.H., Morgan, P., 1990. Continental extension, magmatism and elevation; formal relations and rules of thumb. Tectonophysics 174, 39–62. http://dx.doi.org/10.1016/0040-1951(90)90383-J.

Lester, R., McIntosh, K., Van Avendonk, H.J.A., Lavier, L., Liu, C.-S., Wang, T.K., 2013. Crustal accretion in the Manila trench accretionary wedge at the transition from subduction to mountain-building in Taiwan,. Earth Planet. Sci. Lett. 375, 430–440. http://dx.doi.org/10.1016/j.epsl.2013.06.007.

Lin, J.-Y., Wu, W.-N., Lo, C.-L., 2015. Megathrust earthquake potential of the Manila subduction system as revealed by the seismic moment tensor element Mrr. Terr. Atmos. Ocean. Sci. 26, 619–630. http://dx.doi.org/10.3319/TAO.2013.04.29.01(TC).

McIntosh, K., van Avendonk, H., Lavier, L., Lester, W.R., Eakin, D., Wu, F., Liu, C.-S., Lee, C.-S., 2013. Inversion of a hyper-extended rifted margin in the southern Central Range of Taiwan. Geology 41 (8), 871–874. http://dx.doi.org/10.1130/G34402.1.

Nur, A., Dvorkin, J., Mavko, G., Ben Avraham, Z., 1993. Speculations on the origin and fate of backarc basins. Ann. Geofis. 36, 155–163. http://dx.doi.org/10.4401/ag-4287.

Pilchin, A., 2005. The role of serpentinization in exhumation of high- to ultra-high-pressure metamorphic rocks. Earth Planet. Sci. Lett. 237, 815–828. http://dx.doi.org/10.1016/j.epsl.2005.06.053.

Sibuet, J.-C., Hsu, S.-K., 2004. How was Taiwan created? Tectonophysics 379, 159–181. http://dx.doi.org/10.1016/j.tecto.2003.10.022.

Tan, E., 2017. Mantle wedge serpentinization effects on slab dips. Terr. Atmos. Ocean. Sci. 28, 259–269. http://dx.doi.org/10.3319/TAO.2016.09.21.01.

Taylor, B., Hayes, D.E., 1980. The tectonic evolution of the South China Basin. In: Hayes, D.E. (Ed.), The Tectonic and Geologic Evolution of Southeast Asian Seas and Islands. American Geophysical Union Geophysical Monograph, pp. 89–104. http://dx.doi.org/10.1029/GM023p0089.

Teng, L.S., 1990. Geotectonic evolution of late Cenozoic arc-continent collision in Taiwan. Tectonophysics 183, 57–76. http://dx.doi.org/10.1016/0040-1951(90)90188-E.

Wu, F.T., Rau, R.-J., Salzberg, D., 1997. Taiwan orogeny: thin-skinned or lithospheric collision? Tectonophysics 274, 191–220. http://dx.doi.org/10.1016/S0040-1951(96)00304-6.